

Tight Bounds on 3-Neighbor Bootstrap Percolation

by

Abel Emanuel Romer

B.A.Sc., Quest University Canada, 2017

A Thesis Submitted in Partial Fulfillment of the
Requirements for the Degree of

MASTER OF SCIENCE

in the Department of Mathematics and Statistics

© Abel Emanuel Romer, 2022
University of Victoria

All rights reserved. This thesis may not be reproduced in whole or in part, by photocopying or other means, without the permission of the author.

We acknowledge with respect the Lekwungen peoples on whose traditional territory the university stands, and the Songhees, Esquimalt, and WSÁNEĆ peoples whose historical relationships with the land continue to this day.

Tight Bounds on 3-Neighbor Bootstrap Percolation

by

Abel Emanuel Romer

B.A.Sc., Quest University Canada, 2017

Supervisory Committee

Dr. Peter Dukes, Co-Supervisor
(Department of Mathematics and Statistics)

Dr. Jonathan Noel, Co-Supervisor
(Department of Mathematics and Statistics)

ABSTRACT

Table of Contents

Supervisory Committee	ii
Abstract	iii
Table of Contents	iv
List of Tables	vi
List of Figures	vii
Acknowledgements	ix
Dedication	x
Chapter 1 Introduction	1
1.1 Bootstrap Percolation	3
1.1.1 $m(G, 0)$ and $m(G, 1)$	4
1.1.2 $m(G, 2)$	4
1.1.3 $m(G, 3)$	5
1.2 Other Problems	8
1.3 Conceptual Tools for Understanding Bootstrap Percolation	8
1.3.1 Integrality of bounds	8
1.3.2 A different characterization	9
1.3.3 Attributes of $G[V \setminus A]$	9
1.3.4 The lower bound	9
1.3.5 Surface area, optimality, trees, and components	9
1.3.6 The bipartition (and when to violate it)	9
1.3.7 A potentially interesting proof framework	9
1.4 Structure of this Thesis	10
Chapter 2 A Recursive Technique	11

2.1	A Helpful Lemma	11
2.2	Examples and Notation	12
2.3	Regional vs. Temporal Infections	12
Chapter 3	A Tight Bound on Grids of Size ≥ 5	13
3.1	Introduction and Definitions	13
3.2	Completeness of Thickness 5	13
3.3	Completeness of Thickness 6	15
3.4	Completeness of Thickness 7	16
3.5	Completeness of Grids of Size ≥ 5	18
Chapter 4	Constructions	19
4.1	Introduction	19
4.2	Useful lemmas and observations	19
4.3	Thickness 1	20
4.3.1	Purina	21
4.3.2	Snakes	21
4.4	Thickness 2	23
4.5	Thickness 3	26
4.6	Individual constructions	28
Chapter 5	Torus	32
5.1	Introduction	32
Bibliography		34

List of Tables

Table 1.1	A summary of known bootstrap percolation results for grids and the torus, $r \in \{0, 1, 2, 3, d\}$	4
Table 1.2	Integrality of grids by congruence class. Green indicates integral surface area bound.	9

List of Figures

Figure 1.1	An arbitrary set of initially infected cells in the 10×10 lattice, and the stages of infection.	1
Figure 1.2	Two lethal sets and their resulting infections after one time-step.	2
Figure 1.3	Tight constructions for lethal sets on the $[a] \times [b]$ grid.	5
Figure 2.1	A recursively constructed $[b_1] \times [b_2] \times [b_3]$ grid, for $n = 2$, $d = 3$.	12
Figure 3.1	Thickness 6 grids with perfect percolating sets as obtained in lemma 3.5 (left), and divisibility cases of thickness 6 (right). . .	15
Figure 4.1	A perfect percolating set for $(3, 3, 1)$	21
Figure 4.2	A perfect percolating set for $(15, 15, 1)$	22
Figure 4.3	An optimal percolating set for $(5, 5, 1)$	22
Figure 4.4	An optimal percolating set for $(5, 13, 1)$	22
Figure 4.5	An optimal percolating set for $(11, 13, 1)$	23
Figure 4.6	A perfect percolating set for $(3, 12, 2)$	24
Figure 4.7	A proper unfolding of $G = (3, 12, 2)$. Colored rectangles indicate faces of G . Dashed lines indicate that cells appear on different layers.	24
Figure 4.8	A percolating set on the proper unfolding of $G = (3, 12, 2)$	24
Figure 4.9	A perfect percolating set for $(11, 20, 2)$	25
Figure 4.10	A proper unfolding of $G = (11, 20, 2)$. Colored rectangles indicate faces of G . Dashed lines indicate that cells appear on different layers.	25
Figure 4.11	A percolating set on the proper unfolding of $G = (11, 20, 2)$. . .	25
Figure 4.12	A perfect percolating set for $(12, 21, 2)$	27
Figure 4.13	A proper unfolding of $G = (12, 21, 2)$. Colored rectangles indicate faces of G . Dashed lines indicate that cells appear on different layers.	27
Figure 4.14	A percolating set on the proper unfolding of $G = (12, 21, 2)$. . .	27

Figure 4.15	A percolating set on the proper unfolding H' of $G = (15, 23, 3)$.	28
Figure 4.16	A proper unfolding of $G = (15, 23, 3)$. Colored rectangles indicate faces of G .	28
Figure 4.17		29
Figure 4.18		30
Figure 4.19		31

ACKNOWLEDGEMENTS

DEDICATION

Chapter 1

Introduction

Consider the lattice depicted in the leftmost diagram of Figure 1.1. We refer to the elements of this lattice as *cells*. Suppose we have the capacity to infect some cells (colored red) with a disease, and that this disease will, over a period of time, propagate through uninfected cells of the lattice. Let uninfected cells become infected if they are exposed to at least two infected neighboring cells in the vertical and/or horizontal directions. We say that the initial infection is *lethal* if the entire lattice ultimately becomes infected. Here is the puzzle:

Question. *What is the fewest number of infected cells necessary to spawn a lethal infection?*

Before we present the solution, let us take a moment to examine some properties of infectious sets and attempt to characterize what attributes might correspond to lethality. It should not take too long to observe that if an initial infection is in some way “spread too thin,” it will be unable to jump between infected areas, leading to gaps in infection, which we refer to as *immune regions*. The perimeter of the lattice is particularly susceptible to this, as vertices there have fewer neighbors from whom they might be exposed. Heuristically, then, a lethal set must have the ability to effectively span the entire lattice, and must be particularly virulent along the perimeter.

With this criteria in mind, we are able to make some educated guesses regarding the specific structure of sets that are likely to be lethal. In particular, we would like to consider the two starting infections illustrated in Figure 1.2. Notice that while Figure



Figure 1.1: An arbitrary set of initially infected cells in the 10×10 lattice, and the stages of infection.



Figure 1.2: Two lethal sets and their resulting infections after one time-step.

1.2 (b) has far fewer perimeter infections, both (a) and (b) manage to form continuous bands of infected cells that appear to span the entire lattice after one step. Indeed, this holds with our notion of immune regions (or lack thereof), and we see that both infections will continue to propagate outwards from these bands until all cells become infected.

It is clear from Figure 1.2 that we may obtain lethal sets on the $n \times n$ lattice of size n by simply infecting the diagonal. What is less obvious is whether it is possible to improve upon this result. Perhaps the most natural first attempt at this is to remove an infection from one of the cells along the diagonal. However, this seems to form an immune region around the removed cell. After some experimentation, one begins to believe it impossible to simultaneously satisfy the heuristic that a starting infection must span the lattice, while also using fewer than n initial infections. The question therefore becomes: how do we prove it?

Consider the cumulative perimeter of infected regions. For a given infectious set A , let $P(A)$ be the total perimeter of the infected regions of A . Let A_0 be an initial infection, and observe that $P(A_0) \leq 4|A_0|$. (This bound is only tight if no two infected cells are adjacent. Otherwise, the edge between such cells lies within the infected region, and cannot contribute to the infection's perimeter.) Observe that for any uninfected cell to become infected, it must abut at least two infected cells. Upon infection, the edges adjacent to these cells no longer lie on the infection's perimeter; additionally, the remaining edges of this newly infected cell contribute at most 2 to this perimeter. All told, after infection, $P(A_1) \leq P(A_0)$.

If we suppose that A_0 is a lethal set, then at some point in time, the entire grid will become infected. This infection will have a perimeter $4n$. Since this perimeter did not increase, A_0 must have originally had a perimeter of at least $4n$. Since each cell in A_0 can contribute at most 4 to this perimeter, it must be the case that $|A_0| \geq n$. Our diagonal construction shows that $|A_0| \leq n$, and so we are able to conclude that n is best possible.

This proof is an instance of the famous *perimeter argument*, which has belonged to bootstrap percolation folklore since at least the work of Pete [?]. In the following

section, we present generalizations of this argument to higher dimensional rectangular grids.

1.1 Bootstrap Percolation

The study of such cellular infection spread in grids (and more generally in graphs) is known in the literature as *bootstrap percolation*, and was introduced in the 1970s by Chalupa et al. [2] as a simplified model for the behavior of ferromagnetic fields. In their original 1979 paper, the authors research the stable structure of probabilistically selected initial infections. While this differs from the problem posed in Question 1, the rules for the spread of infection and its broad behavior remain the same. It is worth noting that a large portion of contemporary research on bootstrap problems is focused on questions of probabilistic nature; while these problems are certainly interesting and of merit, they do not fall within the scope of this thesis. Rather, we shall focus on those problems where we have specific control over the structure of the initial infections; in particular, we aim to determine the smallest lethal set on the Cartesian product of paths and cycles.

We define the problem in concrete terms. Let G be a graph and $A_0 \subseteq V(G)$ be a set of initially infected vertices. Iteratively, infect those vertices of G with at least r infected neighbors. For all $t > 0$, let A_t be the set of infected vertices at time step t . We then have

$$A_t = A_{t-1} \cup \{v \in V(G) : |N_G(v) \cap A_{t-1}| \geq r\},$$

where $N_G(v)$ is the set of vertices adjacent to v in G . We define the *closure* of A_0 under r -neighbor bootstrap percolation to be $[A_0] = \bigcup_{t=0}^{\infty} A_t$. We say that A_0 *percolates* or is *lethal* if $[A_0] = V(G)$. We define the smallest percolating set on a graph G under r -neighbor bootstrap percolation by the quantity $m(G, r)$. We note that under these rules, it is not possible for vertices to become uninfected.

While it is possible to study bootstrap percolation on any graph G , most contemporary research focuses on multidimensional grids [?]. We therefore introduce the following notation. For all $n \in \mathbb{N}$, let $[n] = \{1, 2, \dots, n\}$. Let the grid graph with vertex set $\prod_i^d [a_i]$ be denoted by $\prod_i^d [a_i]$. Note that $\prod_i^d [a_i] = P_{a_1} \square \dots \square P_{a_d}$. Furthermore, define:

$$m(a_1, \dots, a_d, r) = m\left(\prod_i^d [a_i], r\right).$$

There are a number of natural generalizations of the problem posed in Question 1. In this thesis, we discuss those obtained by varying the structure of G and the value of r . Below, we outline some of the existing results for graphs that are the Cartesian product of paths and cycles, and $r \in \{0, 1, 2, 3\}$. These results are summarized in Table 1.1.

	Grids								
r	$[a_1]$	$[a_1] \times [a_2]$	$[n]^2$	$[a_1] \times [a_2] \times [a_3]$	$[n]^3$	\cdots	$\prod_{i=1}^d [a_i]$	$[n]^d$	$[2]^d$
$r = 0$	0	0	0	0	0		0	0	0
$r = 1$	1	1	1	1	1		1	1	1
$r = 2$	$\lceil \frac{a_1-1}{2} \rceil + 1$	$\lceil \frac{a_1+a_2-2}{2} \rceil + 1$	n	$\lceil \frac{a_1+a_2+a_3-3}{2} \rceil + 1$	$\lceil \frac{3(n-1)}{2} \rceil + 1$		$\lceil \frac{\sum_{i=1}^d (a_i-1)}{2} \rceil + 1$	$\lceil \frac{d(n-1)}{2} \rceil + 1$	$\lceil \frac{d}{2} \rceil + 1$
$r = 3$???	???	$\lceil \frac{n^2+2n+4}{3} \rceil^*$	S.A. bound	n^2		???	???	$\lceil \frac{d(d+3)}{6} \rceil$
\vdots						\ddots			
$r = d$???	???	???	???	???		S.A. bound	n^{d-1}	???

Table 1.1: A summary of known bootstrap percolation results for grids and the torus, $r \in \{0, 1, 2, 3, d\}$.

1.1.1 $m(G, 0)$ and $m(G, 1)$

In the case where $r \in \{0, 1\}$, the specific structure of G is unimportant. We have the following results:

Theorem 1.1. *For all undirected, simple graphs G , $m(G, 0) = 0$.*

Proof. As cells need not be adjacent to infections to become infected, $A_1 = V(G)$, and so $A_0 = \emptyset$ is lethal. \square

Theorem 1.2. *Let G be an undirected, simple graph with c components. Then $m(G, 1) = c$.*

Proof. Let A_0 be lethal. As infections spread along all edges, it is both necessary and sufficient for each connected component of G to contain exactly one vertex of A_0 . Therefore, $|A_0| = m(G, 1) = c$. \square

1.1.2 $m(G, 2)$

We consider three classes of generalizations: the Cartesian product of paths, the Cartesian product of cycles, and the Cartesian product of both.

Grid: $P_a \square P_b$

Recall from the discussion of Question 1 that $m(n, n, 2) = n$, where the tight construction for the lower bound is given by a diagonal infection expanding laterally outwards. We generalize this result to all rectangular grids.

Theorem 1.3. *For $a, b \geq 1$,*

$$m(a, b, 2) = \left\lceil \frac{a + b - 2}{2} \right\rceil + 1.$$

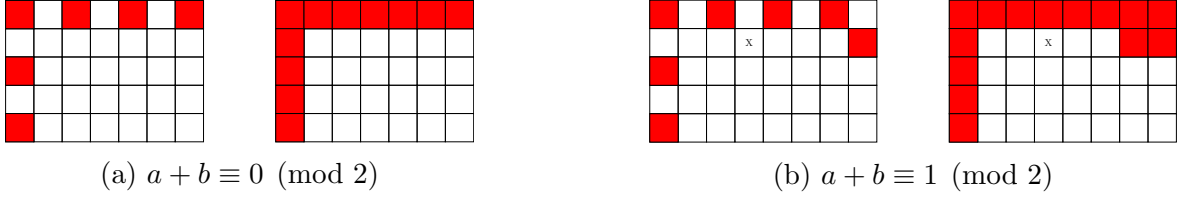


Figure 1.3: Tight constructions for lethal sets on the $[a] \times [b]$ grid.

Proof. We obtain a lower bound on $m(a, b, 2)$ by applying the perimeter argument. Note that the perimeter of the $a \times b$ grid is $2(a + b)$, and so the $m(a, b, 2) \geq \lceil \frac{a+b}{2} \rceil = \lceil \frac{a+b-2}{2} \rceil + 1$. (We take the ceiling because the size of infected sets must be integral.) For the upper bound, we generalize the construction illustrated in Figure 1.2a to rectangular grids. Consider two cases: $a + b \equiv 0 \pmod{2}$ and $a + b \equiv 1 \pmod{2}$ (see Figure 1.3). Note that in both cases, the initial infectious set A_0 is lethal. Furthermore, note that in Figure 1.3a, $|A_0| = \frac{a+b}{2}$, and in Figure 1.3b, $|A_0| = \lceil \frac{a+b}{2} \rceil$. In both cases, this agrees with the perimeter bound. \square

It is worth noting that the integrality condition on the perimeter bound corresponds exactly to the non-existence of cells that are infected by more than two neighbors. In Figure 1.3a, each cell is infected by exactly two neighboring cells; this condition ensures that $P(A_i) = P([A_0])$ for all i . Conversely, in Figure 1.3b, the cell demarcated with an “X” experiences infection on three sides. The existence of such a cell is guaranteed by the fact the perimeter bound in this case is non-integral.

Grid: $P_a \square P_b \square \dots \square P_d$

In a paper by Balogh and Bollobas [1], the above result is generalized to all d -dimensional hypercubes (a_1, \dots, a_d) , $a_i \geq 1$.

Theorem 1.4. *For $d \geq 1$ and $a_1, \dots, a_d \geq 1$,*

$$m(a_1, \dots, a_d, 2) = \left\lceil \frac{\sum_{i=1}^d (a_i - 1)}{2} \right\rceil + 1.$$

1.1.3 $m(G, 3)$

We discuss a further generalization of the perimeter argument to higher dimensions. We show that this argument allows us to obtain nice bounds on 3-neighbor percolation in two and three-dimensional grids. We give a lower bound on the size of lethal sets in the 3-torus and 4-torus. We highlight the main theorem of this thesis.

Grid: $P_n \square P_n$

In 2021, Benevides et al. proved that

$$m(n, n, 3) = \left\lceil \frac{n^2 + 2n + 4}{3} \right\rceil$$

for even n , and

$$\left\lceil \frac{n^2 + 2n}{3} \right\rceil \leq m(n, n, 3) \leq \left\lceil \frac{n^2 + 2n}{3} \right\rceil + 1$$

for odd n . Additionally, they showed that these bounds are tight for odd n : if $n \equiv 5 \pmod{6}$, or $n = 2^k - 1$ for some $k \in \mathbb{N}$, then $m(n, n, 3) = \lceil \frac{n^2 + 2n}{3} \rceil$; and if $n \in \{9, 13\}$, then $m(n, n, 3) = \lceil \frac{n^2 + 2n}{3} \rceil + 1$. Constructions that achieve this bound are illustrated in Chapter 5. We add to this picture with the following theorem, proven in Chapter X, and corollary:

Theorem 1.5. *Suppose that $a, b \geq 1$ such that*

$$m(a, b, 3) = \frac{2ab + a + b}{3}.$$

Then there exists $k \geq 1$ such that $a = b = 2^k - 1$.

Corollary 1.6. *For all $n \geq 1$,*

$$m(n, n, 3) = \begin{cases} \left\lceil \frac{n^2 + 2n + 4}{3} \right\rceil & n \equiv 0 \pmod{2} \\ \frac{n^2 + 2n}{3} & n = 2^k - 1, k \in \mathbb{N} \\ \frac{n^2 + 2n + 1}{3} & n \equiv 5 \pmod{6} \\ \frac{n^2 + 2n + 3}{3} & \text{otherwise.} \end{cases}$$

Proof. The first three cases follow from Theorem 1 of [?] and the observation that if $n \equiv 5 \pmod{6}$, then $\lceil \frac{n^2 + 2n}{3} \rceil = \frac{n^2 + 2n + 1}{3}$. In the final case, n is congruent to either 1 or 3 modulo 6. This implies that $n^2 + 2n$ is divisible by three. From Theorem 1 of [?], we have that $m(n, n, 3) \leq \frac{n^2 + 2n + 3}{3}$. Furthermore, since n is not of the form $2^k - 1$, it follows from Theorem 1.5 that $m(n, n, 3) > \frac{n^2 + 2n}{3}$. Therefore, $m(n, n, 3) = \frac{n^2 + 2n + 3}{3}$. \square

This result resolves the question of the minimum lethal set for two dimensional square grids. For the more general case of rectangular grids, the problem remains unsolved. However, we are able to achieve an upper bound of $m(a, b, 3) \leq \lceil \frac{ab + a + b + 6}{3} \rceil$ for all $a, b > 1$. Further discussion of these results can be found in Chapter X.

Grid: $P_a \square P_b \square P_c$

Surprisingly, it is possible to extend the perimeter argument to higher dimensions [?]. This provides a lower bound on $m(a_1, a_2, a_3, 3)$ of $\lceil \frac{a_1 a_2 + a_2 a_3 + a_1 a_3}{3} \rceil$. We refer to this quantity as the *surface area bound*. In Chapters 2 and 3, we use a recursive strategy to prove that the surface area bound is met for all sufficiently large grids.

Theorem 1.7. *For all $a_1, a_2, a_3 \geq 11$,*

$$m(a_1, a_2, a_3, 3) = \left\lceil \frac{a_1 a_2 + a_2 a_3 + a_1 a_3}{3} \right\rceil.$$

Grid: $P_a \square P_b \square \dots \square P_d$

Do we have a bound here?

Torus: $C_a \square C_b$

A lower bound for the Cartesian product of two cycles is given in Benevides [?]. Their proof is included here for completeness.

Theorem 1.8. *For $a, b \geq 1$,*

$$m(C_a \square C_b, 3) \geq \left\lceil \frac{ab + 1}{3} \right\rceil.$$

Proof. Let $G = C_a \square C_b$, and let I be a lethal set on G . Let $H = V(G) \setminus I$, and note that $|H| = ab - |I|$. Let m_H be the number of edges in the subgraph of G induced by H , and m_{IH} be the number of edges between vertices in I and vertices in H . Note that m_{IH} is similar to the notion of perimeter on a grid.

Observe that $G[H]$ must be cycle-free: cycles in $G[H]$ constitute immune regions, and contradict the lethality of I . Therefore, $G[H]$ is a forest, and so $m_H = |H| - c$, where c is the number of components in $G[H]$. Additionally, note that $m_{IH} \leq 4|I|$, since G is 4-regular. Finally, observe that the total degree of $G[H]$ is $2m_H = 4|H| - m_{IH}$.

Chaining together these inequalities, we obtain:

$$\begin{aligned} 4|I| &\geq m_{IH} = 4|H| - 2m_H \\ &= 4|H| - 2(|H| - c) = 2|H| + 2c \\ &= 2(ab - |I|) + 2c \end{aligned}$$

Combining like terms and simplifying, we have

$$|I| \geq \frac{ab + c}{3} \geq \frac{ab + 1}{3}.$$

□

Observe that the conditions $c \geq 1$ and $m_{IH} \leq 4|I|$ prevent us from obtaining strict equality. Specifically, if I is lethal, $G[H]$ has one component, and no vertices in I are adjacent, then $|I|$ is minimized.

Torus: $C_a \square C_b \square C_c$

Present the lower bound and note that we are able to obtain constructions within constant distance of this bound for arbitrarily large grids.

1.2 Other Problems

In this section, we provide a cursory overview of some other related areas of study in bootstrap percolation. We highlight problems regarding the number of iterations necessary to infect all vertices on a graph.

1.3 Conceptual Tools for Understanding Bootstrap Percolation

As outlined above, it appears that lethal sets in grid graphs adhere to certain fixed rules. We examine these rules here, and explain why they are necessary and helpful for understanding the problem of bootstrap percolation.

1.3.1 Integrality of bounds

Not all grids have integral surface area bounds. We refer to such grids as *non-divisibility cases*. The non-divisibility cases for three-dimensional grids where $r = 3$ are illustrated in red in Table 1.2.

Percolation in non-divisible grids is inefficient in one of two ways: either each vertex in A_0 contributes, on average, less than $2d$ units to the final surface area, or at some time-step i , there exists a vertex $v \in V \setminus A_i$ such that $N_{A_i}(v) > r$. In the first case, the inefficiency is a consequence of two adjacent vertices in A_0 ; heuristically, we may view this as poor distribution of infection across the grid. In the second case, the inefficiency results from excessive infection in a particular region; a vertex is over-exposed.

It is insightful to consider this behavior in the context of Theorem 1.8. Instead of thinking of m_{IH} at the number of edges between I and H , we shall consider it to represent the perimeter, or surface area, of the initial infection I .

mod 3	$a_1 \equiv 0$	$a_1 \equiv 1$	$a_1 \equiv 2$
$a_2 \equiv 0$			
$a_2 \equiv 1$			
$a_2 \equiv 2$			

(a) $a_3 \equiv 1 \pmod{3}$

mod 3	$a_1 \equiv 0$	$a_1 \equiv 1$	$a_1 \equiv 2$
$a_2 \equiv 0$			
$a_2 \equiv 1$			
$a_2 \equiv 2$			

(b) $a_3 \equiv 2 \pmod{3}$

mod 3	$a_1 \equiv 0$	$a_1 \equiv 1$	$a_1 \equiv 2$
$a_2 \equiv 0$			
$a_2 \equiv 1$			
$a_2 \equiv 2$			

(c) $a_3 \equiv 0 \pmod{3}$

Table 1.2: Integrality of grids by congruence class. Green indicates integral surface area bound.

1.3.2 A different characterization

We shall find it useful to think about the problem of bootstrap percolation in terms of the graph induced by the set of uninfected vertices $V \setminus A_i$ at some time-step t_i .

1.3.3 Attributes of $G[V \setminus A]$

No cycles, no paths between opposite faces. Reference to Benevides.

1.3.4 The lower bound

Let us reconsider the our proof of the lower bound in this new framework.

1.3.5 Surface area, optimality, trees, and components

The surface area bound is not always integral. In cases where it is not, this sub-optimality can be traced to a particular time-step where an uninfected cell is infected by more than r neighbors. The proof of the lower bound on the torus considers the number of components in $T[V \setminus A]$, as each such component necessarily collapses in on a vertex where this occurs. In the grid, this circumstance can be avoided by permitting components to abut the perimeter. What is the relationship here?

1.3.6 The bipartition (and when to violate it)

Discuss the heuristic of placing infections on one side of the bipartition and when this technique fails.

1.3.7 A potentially interesting proof framework

A discussion on the broad structure of the proof of the lower bound on the torus as presented in Benevides. Note that this proof relies on a sequence of inequalities, and that two of these inequalities characterize precise conditions that are necessary for a set to be lethal. Discuss how the proof might change as a function of the dimension of the grid.

1.4 Structure of this Thesis

In the following chapter, we lay out in formal terms those lemmas necessary to understand and prove Theorem 1.7. In particular, we discuss the recursive technique that permits the construction of lethal sets on grids of arbitrary large size, as well as a number of characteristics of lethal sets. We distinguish between two types of grids—those with integral *SA bound*, and those without—and show that it is possible obtain tight constructions on non-integral grids from integral grids.

In Chapter 3, we prove that there exist lethal sets at the S.A. bound for all integral grids of size at least 5. This chapter makes significant use of a number of existing constructions, described in Chapter 6, as well as the recursive strategy introduced in Chapter 2.

Chapter 4 extends the results of Chapter 3 to all grids of size at least 11 with non-integral surface area bound.

Chapter 5 considers the specific case of grids of the form $(a, b, 1)$, and answers a question posed in Benevides et al. [?] regarding the existence of tight lethal sets on non-square grids.

Chapter 6 is dedicated to presenting and proving the lethality of sets on a number of grids, and families of grids.

Chapter 7 discusses some of the programmatic techniques used to evaluate, examine and explore the behavior of percolating sets.

Chapter 8 examines the problem of bootstrap percolation on the 3- and 4-torus, and presents a class of constructions within constant size of the lower bound.

Chapter 9 presents open questions related to the results presented in this thesis, and provides some suggestions for future research.

Chapter 2

A Recursive Technique

In this chapter, we shall present a technique for constructing large *perfect* grids from smaller perfect grids.

2.1 A Helpful Lemma

Note that there are certain broad structures in a cube that, if present, immediately guarantee it become fully infected. Of greatest importance here is the observation that certain configurations of fully infected sub-cubes (which we shall call blocks) will cause the larger brick to become infected.

Furthermore, note that if each of these smaller blocks is infected with a minimum lethal set, the composite larger brick will also be infected with a minimum lethal set (barring some considerations for divisibility).

The proof of this claim makes use of the so-called *modified bootstrap process* in $[n]^d$, discussed in [?] and [?]. This is a strengthened variation of the problem introduced in the previous chapter, whereby vertices in the $[n]^d$ grid become infected if and only if they are adjacent to infected vertices along edges in each of the d directions. For example, in the $[n]^2$ grid, a vertex that sees infection in one of both the North/South and East/West directions will itself become infected, whereas a vertex with infected neighbors to the East and West (but not North and South) will not.

In particular, the lemma considers composite grids $[n]^d$ where each vertex $x = (x_1, \dots, x_d) \in [n]^d$ is itself a smaller block G_x . We prove that lethal sets on these grids can be built from the smaller lethal sets on each G_x .

Lemma 2.1. *For $n, d \geq 1$, let $A = (a_{i,j})$ be a $d \times n$ matrix of positive integers, and let $b_i = \sum_{j=1}^n a_{i,j}$, for $1 \leq i \leq d$. Let S be a lethal set under the modified process on $[n]^d$, and for each vertex $\vec{x} = (x_1, \dots, x_d) \in S$, let $T_{\vec{x}}$ be a lethal set on $\prod_{i=1}^d [a_{i,x_i}]$ under d -neighbor percolation. Then*

$$m(b_1, \dots, b_d, d) \leq \sum_{\vec{x} \in S} |T_{\vec{x}}|.$$

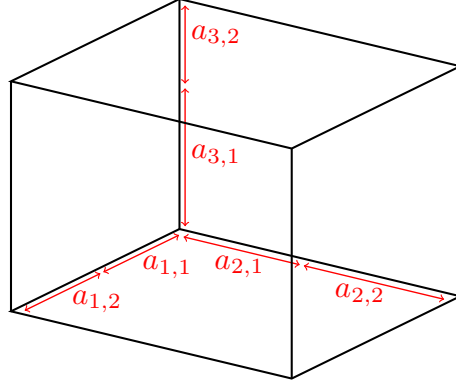


Figure 2.1: A recursively constructed $[b_1] \times [b_2] \times [b_3]$ grid, for $n = 2$, $d = 3$.

Proof. We imagine sub-dividing the $\prod_{i=1}^d [b_i]$ brick into smaller blocks by partitioning each of the d axes into segments $a_{i,1}, a_{i,2}, \dots, a_{i,n}$, $1 \leq i \leq d$. \square

2.2 Examples and Notation

2.3 Regional vs. Temporal Infections

Chapter 3

A Tight Bound on Grids of Size ≥ 5

3.1 Introduction and Definitions

Let the ordered tuple (a, b, c) represent the $a \times b \times c$ grid G where $a \geq b \geq c$. We refer to c as the *thickness* of G . For example, the tuple $(5, 3, 3)$ represents a $5 \times 3 \times 3$ grid of thickness 3. We refer to a tuple as *divisible*, or a *divisibility case*, if and only if $ab + bc + ca \equiv 0 \pmod{3}$. If a tuple is divisible and percolates at the lower bound, we refer to it as *perfect*. Observe that the divisibility cases are precisely those grids with integral lower bounds. The divisibility cases of thicknesses belonging to the three residue classes modulo 3 are illustrated in {Figure something}.

In the following lemmas, we use the notation $(a, b, c) + (x, y, z) = (a + x, b + y, c + z)$ to represent respective increases of x , y , and z to the side lengths a , b , and c of G . We note the following:

Remark 3.1. By applying the recursion, $(a, b, c) + (x, y, z)$ percolates at the lower bound when either:

1. $(a, b, c), (a, y, z), (x, b, z), (x, y, c)$ all percolate at the lower bound; or
2. $(x, y, z), (x, b, c), (a, y, c), (a, b, z)$ all percolate at the lower bound.

We shall call a thickness *complete* if it can be shown that all divisibility cases in that thickness are perfect. In this section, we demonstrate that thickness 5, thickness 6 and thickness 7 are all complete. As these belong to the residue classes 2, 0, and 1 modulo 3, respectively, we then use a recursive construction to show that all larger grids are also complete.

3.2 Completeness of Thickness 5

Leveraging {lemmas from earlier chapters yet to be written}, we show that all divisibility cases in thickness 5 percolate at the lower bound.

NOTE: THE FOLLOWING LEMMAS HOLD ASSUMING WE HAVE A GENERAL CONSTRUCTION FOR $(2, 3, 3k)$ FOR ALL k .

Lemma 3.2. *All divisibility cases for grids of the form $(k, 5, 5)$ are perfect.*

Proof. We consider grids obtained from $(5, 2, 2) + (a, 3, 3)$, for $a \equiv 0 \pmod{3}$ and $a > 3$. By remark 3.1, it is sufficient to show that $(5, 2, 2)$, $(5, 3, 3)$, $(a, 2, 3)$, $(a, 2, 3)$ are all perfect. By {a bunch of constructions}, each of these grids percolates at the lower bound for $a > 3$. We therefore obtain all grids of the form $(k, 5, 5)$, for $k > 8$. The only missing grids are $(5, 5, 5)$ and $(8, 5, 5)$, which we have by construction. This completes the proof. \square

Lemma 3.3. *All divisibility cases for grids of the form $(k, 6, 5)$ percolate at the lower bound.*

Proof. We consider grids obtained from $(6, 3, 2) + (a, 3, 3)$, for $a \equiv 0 \pmod{3}$ and $a > 3$. By remark 3.1, it is sufficient to show that $(6, 3, 2)$, $(6, 3, 3)$, $(a, 3, 3)$, $(a, 3, 2)$ are all perfect. By {a bunch of constructions}, each of these grids percolates at the lower bound for $a > 3$. We therefore obtain all grids of the form $(k, 6, 5)$, for $k > 8$. The only missing grid is $(6, 6, 5)$, which we have by construction. This completes the proof. \square

Lemma 3.4. *Thickness 5 is complete.*

Proof. Let $(a, b, 2)$ represent an arbitrary (divisible) grid of thickness 2, and let $x = a \pmod{6}$ and $y = b \pmod{6}$. By {some as of yet unwritten construction}, we have that $(a, b, 2)$ percolates at the lower bound for all $x, y \in \{0, 2, 3, 5\}$, where $x \neq y$. We consider two constructions: $(a, b, 2) + (6, 3, 3)$ and $(a, b, 2) + (6, 6, 3)$.

By item (1) of the remark, in order to show that $(a, b, 2) + (6, 3, 3)$ percolates at the lower bound, it is sufficient to show that $(a, b, 2)$, $(a, 3, 3)$, $(6, b, 3)$, $(6, 3, 2)$ all percolate at the bound. By {more unwritten constructions}, this is true for all $x, y \in \{0, 2, 3, 5\}$, where $x \neq y$, $a, b > 1$, and at least one of $\{a, b\} > 2$. (Note that if $a = 2$, one of the tuples is $(2, 3, 3)$, which does not percolate at the lower bound; we accommodate for this by re-writing $(a, b, 2) + (6, 3, 3)$ as $(a, b, 2) + (3, 6, 3)$.) The resulting tuple $(a', b', 5)$ is a grid of thickness 5, with a' and b' in the same residue class modulo 6, $x, y \geq 8$, and at least one of $\{a', b'\} \geq 9$. From {some figure representing the divisibility cases of thickness 5}, we see that the lower bound on a' and b' omits all grids of the form $(5, 5, k)$ and $(5, 6, k)$, as well as the singular grid $(8, 8, 5)$.

Applying an analogous argument to $(a, b, 2) + (6, 6, 3)$, we must demonstrate that $(a, b, 2)$, $(a, 6, 3)$, $(6, b, 3)$, $(6, 6, 2)$ all percolate at the lower bound. By {some other constructions}, we again find that this holds for all $x, y \in \{0, 2, 3, 5\}$, where $x \neq y$ and $a, b > 1$. This gives all thickness 5 tuples $(a', b', 5)$ with a' and b' in different residue classes modulo 6, where $a', b' \geq 8$.

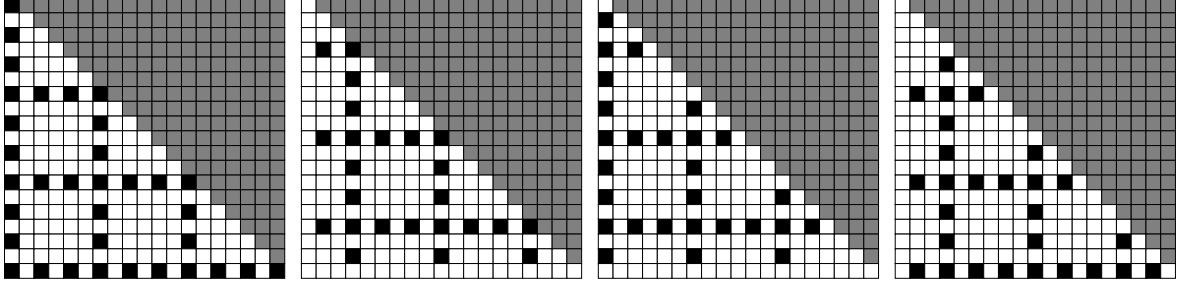


Figure 3.1: Thickness 6 grids with perfect percolating sets as obtained in lemma 3.5 (left), and divisibility cases of thickness 6 (right).

Combining these results, we have completeness for all grids of thickness 5 except those of the form $(5, 5, k)$ and $(5, 6, k)$, and the singular grid $(8, 8, 5)$. By lemmas 3.2 and 3.3, and $\{\text{some construction for } (8, 8, 5)\}$, these cases are also complete, and so thickness 5 is complete. This completes the proof. \square

3.3 Completeness of Thickness 6

We shall show that all grids of thickness 6 can be obtained recursively from $(3n, m, 3)$, where $n, m \equiv 1 \pmod{2}$ (this is that general thickness 3 construction), and one of $\{(3, 3, 3), (6, 6, 3), (6, 3, 3), (3, 6, 3)\}$. We examine each of these cases separately and show that each is complete.

(NOTE (to Peter and Jon): I have struggled a bit with the canonical way to describe grids. I like the tuple representation (a, b, c) where WLOG $a \leq b \leq c$. However, this becomes a bit mucky in the following proofs, because $(3n, m, 3)$ potentially violates this rule if n is large and m is small. To accommodate this, I have written “grids of the form $(a, b, 6)$, where $a \equiv 0 \pmod{6}$ and $b \equiv 0 \pmod{2}$, or $b \equiv 0 \pmod{6}$ and $a \equiv 0 \pmod{2}$,” in an attempt to address the circumstance where the ordering of the tuple is flipped because n is large and m is small. However, I think this may just muddy the waters.)

Lemma 3.5. *All grids of the form $(a, b, 6)$, where $a \equiv 0 \pmod{6}$ and $b \equiv 0 \pmod{2}$, or $b \equiv 0 \pmod{6}$ and $a \equiv 0 \pmod{2}$, percolate at the lower bound.*

Proof. We consider $(3n, m, 3) + (3, 3, 3)$, for $n, m \equiv 1 \pmod{2}$. By remark 3.1, we have that $(3n, m, 3) + (3, 3, 3)$ percolates if $(3n, m, 3), (3n, 3, 3), (3, m, 3), (3, 3, 3)$ all percolate. By construction {yet to be named}, all grids $(a, 3, 3)$ are perfect. Therefore, $(3, 3n, m) + (3, 3, 3)$ is perfect. Note that this grid is of the form $(3k, l, 6)$, where $k, l \equiv 0 \pmod{2}$. This is equivalent to grids of the form $(a, b, 6)$, where $a \equiv 0 \pmod{6}$ and $b \equiv 0 \pmod{2}$, or $b \equiv 0 \pmod{6}$ and $a \equiv 0 \pmod{2}$. This completes the proof. \square

Lemma 3.6. *All grids of the form $(a, b, 6)$, where $a \equiv 3 \pmod{6}$ and $b \equiv 1 \pmod{2}$, or $b \equiv 3 \pmod{6}$ and $a \equiv 1 \pmod{2}$, percolate at the lower bound.*

Proof. We apply the same argument as above, this time considering $(3n, m, 3) + (6, 6, 3)$, for $n, m \equiv 1 \pmod{2}$. Again, by remark 3.1, it is sufficient to show that $(3n, m, 3), (3n, 6, 3), (6, m, 3), (6, 6, 3)$ are all perfect. By {more thickness 3 constructions}, each of these grids percolates at the lower bound. The resulting grid, $(3n, m, 3) + (6, 6, 3)$, for $n, m \equiv 1 \pmod{2}$, is of the form $(a, b, 6)$, for $a \equiv 3 \pmod{6}$ and $b \equiv 1 \pmod{2}$, or $b \equiv 3 \pmod{6}$ and $a \equiv 1 \pmod{2}$. This completes the proof. \square

Lemma 3.7. *All grids of the form $(a, b, 6)$, where $a \equiv 3 \pmod{6}$ and $b \equiv 0 \pmod{2}$, or $b \equiv 3 \pmod{6}$ and $a \equiv 0 \pmod{2}$, percolate at the lower bound.*

Proof. Similarly to the previous proofs, we consider $(3n, m, 3) + (6, 3, 3)$, for $n, m \equiv 1 \pmod{2}$. We show that $(3n, m, 3), (3n, 3, 3), (6, m, 3), (6, 3, 3)$ are all perfect. By the same thickness 3 constructions, each of these grids percolates at the lower bound. Therefore, by remark 3.1, $(3n, m, 3) + (6, 3, 3)$ is perfect. Furthermore, observe that $(3n, m, 3) + (6, 3, 3)$ is of the form $(a, b, 6)$, where $a \equiv 3 \pmod{6}$ and $b \equiv 0 \pmod{2}$. This completes the proof. \square

Lemma 3.8. *All grids of the form $(a, b, 6)$, where $a \equiv 0 \pmod{6}$ and $b \equiv 1 \pmod{2}$, or $b \equiv 0 \pmod{6}$ and $a \equiv 1 \pmod{2}$, percolate at the lower bound.*

Proof. We consider $(3n, m, 3) + (3, 6, 3)$, for $n, m \equiv 1 \pmod{2}$. We show that $(3n, m, 3), (3n, 6, 3), (3, m, 3), (3, 6, 3)$ are all perfect. By {thickness 3 constructions} and remark 3.1, $(3n, m, 3) + (3, 6, 3)$ is perfect. Observe that $(3n, m, 3) + (3, 6, 3)$ is of the form $(a, b, 6)$, where $a \equiv 0 \pmod{6}$ and $b \equiv 1 \pmod{2}$. This completes the proof. \square

Lemma 3.9. *Thickness 6 is complete.*

Proof. All divisibility cases for thickness 6 are grids of the form $(x, y, 6)$ such that at least one of $\{x, y\}$ is congruent to 0 modulo 3. Lemmas 3.5, 3.6, and 3.7 cover all such cases. The result follows. \square

3.4 Completeness of Thickness 7

We show that all divisibility cases for grids of thickness 7 percolate at the lower bound. Observe that divisibility cases for thickness 7 consist of grids of the form $(x, y, 7)$ for x, y in residue classes $\{0, 1, 3, 4\}$ modulo 6. We separate these divisibility cases into the following four categories and show that each category is complete:

1. $(x, y, 7)$ for $x, y \in \{1, 4\}$ and $x \equiv y \pmod{6}$;
2. $(x, y, 7)$ for $x, y \in \{1, 4\}$ and $x \not\equiv y \pmod{6}$;

3. $(x, y, 7)$ for $x, y \in \{0, 3\}$ and $x \equiv y \pmod{6}$;
4. $(x, y, 7)$ for $x, y \in \{0, 3\}$ and $x \not\equiv y \pmod{6}$.

Lemma 3.10. *All grids of the form $(x, y, 7)$ for $x, y \in \{1, 4\}$ and $x \equiv y \pmod{6}$ are complete.*

Proof. Consider the construction $(a, b, 2) + (8, 5, 5)$ for $a, b \in \{2, 5\}$ and $a \not\equiv b \pmod{6}$. Observe that this construction obtains all grids of the form described in (1) above. We show that the grids $(a, b, 2), (a, 5, 5), (8, b, 5), (8, 5, 2)$ are all complete. {The fact that these grids are complete follows from a number of constructions and the observation that thickness 5 is complete.} By remark 3.1, the construction $(a, b, 2) + (8, 5, 5)$ percolates at the lower bound. This completes the proof. \square

Lemma 3.11. *All grids of the form $(x, y, 7)$ for $x, y \in \{1, 4\}$ and $x \not\equiv y \pmod{6}$ are complete.*

Proof. Consider the construction $(a, b, 2) + (5, 5, 5)$ for $a, b \in \{2, 5\}$ and $a \not\equiv b \pmod{6}$. Observe that this construction obtains all grids of the form described in (2) above. We consider the grids $(a, b, 2), (a, 5, 5), (5, b, 5), (5, 5, 2)$. By {known constructions and completeness of thickness 5}, each of these grids is perfect, and so by remark 3.1, $(a, b, 2) + (5, 5, 5)$ percolates at the lower bound. This completes the proof. \square

Lemma 3.12. *All grids of the form $(x, y, 7)$ for $x, y \in \{0, 3\}$ and $x \equiv y \pmod{6}$ are complete.*

Proof. Consider the construction $(a, b, 2) + (6, 9, 5)$ for $a, b \in \{0, 3\}$ and $a \not\equiv b \pmod{6}$. Observe that this construction contains all grids described in (3) above. We consider the grids $(a, b, 2), (a, 9, 5), (6, b, 5), (6, 9, 2)$. Observe that $(3, 9, 5)$ is perfect by construction, and $(a, 9, 5)$ is perfect in general for $a > 3$. Similarly, $(6, 3, 5)$ is perfect by construction, and $(6, b, 5)$ is perfect for all other $b > 3$. Finally, $(a, b, 2)$ and $(6, 9, 2)$ are perfect by construction. Therefore, by remark 3.1, $(a, b, 2) + (6, 9, 5)$ percolates at the lower bound. This completes the proof. \square

Lemma 3.13. *All grids of the form $(x, y, 7)$ for $x, y \in \{0, 3\}$ and $x \not\equiv y \pmod{6}$ are complete.*

Proof. Consider the construction $(a, b, 2) + (6, 6, 5)$ for $a, b \in \{0, 3\}$ and $a \not\equiv b \pmod{6}$. Observe that this construction contains all grids described in (4) above. We consider the grids $(a, b, 2), (a, 6, 5), (6, b, 5), (6, 6, 2)$. Observe that $(3, 6, 5)$ is perfect by construction, and $(a, 6, 5)$ is perfect in general for $a > 3$. Similarly, $(6, 3, 5)$ is perfect by construction, and $(6, b, 5)$ is perfect for all other $b > 3$. Finally, $(a, b, 2)$ and $(6, 6, 2)$ are perfect by construction. Therefore, by remark 3.1, $(a, b, 2) + (6, 6, 5)$ percolates at the lower bound. This completes the proof. \square

Lemma 3.14. *Thickness 7 is complete.*

Proof. By lemmas 3.10, 3.11, 3.12, and 3.13, all divisibility cases for thickness 7 percolate at the lower bound. \square

3.5 Completeness of Grids of Size ≥ 5

We can get completeness in every residue class modulo 3 by simply considering the grids obtained from $(x, y, z) + (3, 3, 3)$.

Chapter 4

Constructions

4.1 Introduction

In this chapter, we present diagrammed proofs of lethal sets that percolate at the lower bound. The proofs are organized by the thickness of the grid. Many of the constructions in the following sections belong to infinite families of either optimal or perfect sets. In this case, we shall examine the grids by region, and observe that certain regions can be expanded to arbitrarily large sizes using mathematical induction.

We shall call a thickness *semi-complete* if all divisibility cases are optimal.

4.2 Useful lemmas and observations

We shall see that similar patterns and structures appear with some regularity in optimal sets. These structures always infect entire regions, and it will be helpful to recognize them within larger grids when they appear.

Lemma 4.1. *Let $G = P_a \square P_b$ be a graph and $S \subseteq V(G)$ be a subset of the vertices of G . Let $G[\overline{S}]$ be the subgraph of G induced by vertices not in S . Then S is a lethal set if and only if $G[\overline{S}]$ is cycle-free, and has no paths between any two boundary vertices.*

Lemma 4.2. *Let G be the grid graph (a, b, c) and let A be a set of infected vertices in G . Let $H = G[\overline{A}]$ be the subgraph of G induced by uninfected vertices. Let $\{F, F'\} \subseteq V(G)$ be orthogonal faces of G . If H does not contain a path between vertices $v \in F, v' \in F'$, then G percolates.*

Proof. We proceed by induction on $|V(H)| = abc - |A|$. If $|V(H)| = 0$, then all vertices of G are infected and we are done. Suppose $|V(H)| > 0$, and consider a connected component Y of H . By hypothesis, Y does not contain a path between any two orthogonal faces of G . Therefore, without loss of generality, there exists a face $X = \{a\} \times \{1, \dots, b\} \times \{1, \dots, c\}$ such that $V(Y) \cap X = \emptyset$. Take the largest i such that

$X_i = \{a\} \times \{1, \dots, b\} \times \{1, \dots, c\}$ contains a vertex of Y . Repeat this process to obtain maximal faces Y_j and Z_k in the b and c directions, respectively.

Observe that this construction gives a vertex $v = (i, j, k) \in V(Y)$, and planes $X_{i+1}, Y_{j+1}, Z_{k+1}$ such that $(X_{i+1} \cup Y_{j+1} \cup Z_{k+1}) \cap V(Y) = \emptyset$. In particular, note that $(i+1, j, k), (i, j+1, k), (i, j, k+1) \in N(v)$. Since these three vertices belong to A and $v \notin A$, v becomes infected. Furthermore, since $|V(H) \setminus \{v\}| < |V(H)|$, the resulting graph percolates by induction. This completes the proof. \square

Corollary 4.3. *Let G be the grid graph (a, b, c) . If a set A is lethal on three mutually orthogonal faces of G , then A is lethal on G .*

Proof. Let X, Y, Z be three mutually orthogonal faces of G . By hypothesis, $X \cup Y \cup Z \subseteq A_t$ for some time t . Therefore, the graph $H = G[\overline{A}_t]$ cannot contain a path between vertices on orthogonal faces of G . By lemma 4.2, G percolates. \square

Corollary 4.4. *Let G be the grid graph (a, b, c) and let A be a set of infected vertices of G . Let $\{R_1, \dots, R_k\}$ be a partition of $V(G) \setminus A$ into sub-grids $(a_1, b_1, c_1), \dots, (a_k, b_k, c_k)$ such that each R_i is bounded by a lethal infection on three mutually orthogonal faces. Then A is lethal on G .*

Proof. By hypothesis and corollary 4.3, A is lethal on each R_i . Since $A \cup R_1 \cup \dots \cup R_k = V(G)$ and each R_i becomes infected, A must be lethal. \square

Definition 4.5. Let a *manifold* M of the grid graph $G = (a, b, c)$ be any set of vertices A satisfying the conditions of corollary 4.4.

Definition 4.6. Let a *proper unfolding* of $G = (a, b, c)$ be a planar representation of the manifold of G . This can be thought of as a special type of folding net of G , such that when assembled the resulting structure satisfies the conditions of corollary 4.4.

Corollary 4.7. *Let M be the proper unfolding of a manifold of $G = (a, b, c)$, and let A be a lethal set on M . Then A is lethal on G .*

Proof. The proof follows directly from definitions 4.5 and 4.6. \square

4.3 Thickness 1

There are two general constructions in thickness 1 that percolate at the surface area bound. The first construction is perfect for all $(2^n - 1, 2^n - 1, 1)$ grids, and originates in a 2021 paper by Benevides et al. [?]. The second construction is optimal for all grids $(a, b, 1)$, where $a \equiv 5 \pmod{6}$, $b \equiv 1 \pmod{2}$, and $a, b \geq 5$. As such grids constitute non-divisibility cases, this construction is not perfect.

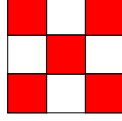


Figure 4.1: A perfect percolating set for $(3, 3, 1)$.

4.3.1 Purina

We refer to this construction colloquially as the Purina construction, due to the similarity between its instance on the $(3, 3, 1)$ grid and the logo of the pet food brand. No funding has been offered, but we are open to the possibility. A more extensive discussion on this pattern can be found in [?].

Construction 4.8. *All grids of the form $(2^n - 1, 2^n - 1, 1)$ are perfect.*

Proof. This is a recursive construction built from the base component piece shown in figure 4.1. Note that this $(3, 3, 1)$ construction is lethal under the 3-neighbor bootstrap process, and that it meets the surface area bound:

$$\frac{1}{3} \cdot (ab + bc + ca) = \frac{1}{3} \cdot (9 + 3 + 3) = 5.$$

For larger grids of size $(2^n - 1, 2^n - 1, 1)$, join four copies of $(2^{n-1} - 1, 2^{n-1} - 1, 1)$ about two perpendicular corridors, and infect the vertex at their intersection (figure 4.2). Observe that the resulting set is lethal: each of the four smaller grids is lethal by hypothesis, and the remaining vertices induce a forest with disconnected boundary points, which percolates by lemma 4.1. Furthermore, note that

$$\begin{aligned} \text{S.A.}(2^n - 1, 2^n - 1, 1) &= \frac{1}{3} \cdot (2^{2n} - 1) \\ &= 4 \cdot \frac{1}{3} \cdot (2^{2n-2} - 1) + 1 = 4 \cdot \text{S.A.}(2^{n-1} - 1, 2^{n-1} - 1, 1) + 1, \end{aligned}$$

and therefore this construction is perfect. \square

4.3.2 Snakes

As indicated by lemma 4.1, a fundamental characteristic of lethal sets S is the presence of an initially uninfected corridor, bounded by walls of infection. This structure is apparent in the second diagrams of figures 4.2 and 4.5. These corridors correspond to forests in the complement $G[\overline{S}]$ of S . In this subsection, we provide a general method for constructing such corridors in $(a, b, 1)$ grids where $a \equiv 5 \pmod{6}$ and $b \equiv 1 \pmod{2}$.

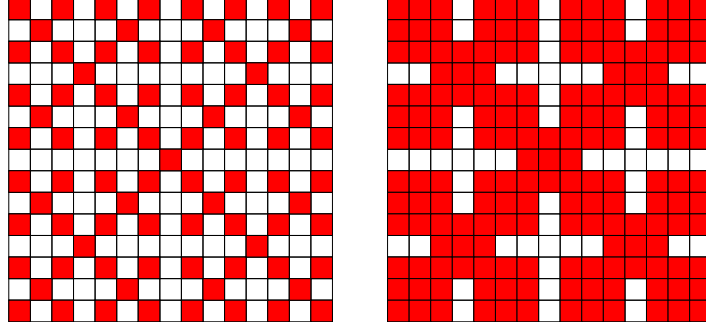


Figure 4.2: A perfect percolating set for $(15, 15, 1)$.

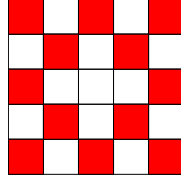


Figure 4.3: An optimal percolating set for $(5, 5, 1)$.

Construction 4.9. All grids of the form $(a, b, 1)$, $a \equiv 5 \pmod{6}$, $b \equiv 1 \pmod{2}$, and $a, b \geq 5$ are optimal.

Proof. For grids of the form $(a, b, 1)$, $a \equiv 5 \pmod{6}$, $b \equiv 1 \pmod{2}$, we construct an optimal infected set and show that it percolates by lemma 4.1. For the base case, consider the $(5, 5, 1)$ grid G illustrated in figure 4.3. Observe that this construction is optimal. Now consider the grid G' resulting from the insertion of a $(5, 2k, 1)$ block, as shown in figure 4.4. Note that the subgraph induced by the uninfected vertices of G' satisfies the conditions of lemma 4.1. Furthermore, note that if any $(5, n, 1)$ grid is optimal, the $(5, n+2, 1)$ grid resulting from such a construction has surface area bound $\text{S.A.}(5, n, 1) + 4$, which agrees with the number of infected vertices.

To extend this construction in the vertical direction, we introduce a kink in the snaking infection. This kink requires six rows to produce a repeating pattern. The structure of this design is shown in figure 4.5. For grids of smaller width, the same construction gives optimal percolating sets; however, the snaking pattern is increasingly difficult to recognize in thin grids. \square

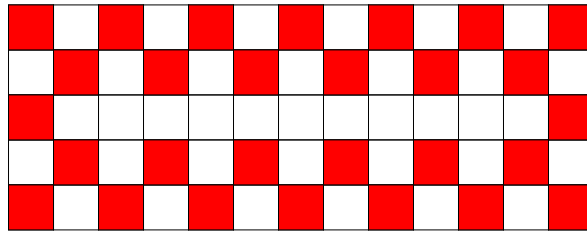


Figure 4.4: An optimal percolating set for $(5, 13, 1)$.

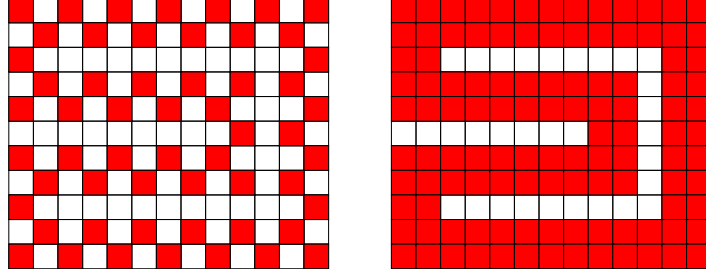


Figure 4.5: An optimal percolating set for $(11, 13, 1)$.

4.4 Thickness 2

In this section we examine four infinite families of perfect grids. We show that each has a manifold that admits a lethal set of perfect size. We note that such lethal sets are likely to exist for nearly all divisibility cases in thickness two; however, constructions are elusive and those presented here are sufficient to prove the main result of this thesis.

Unlike those presented in the previous section, the following proofs all leverage lemma 4.2. As a consequence, their argumentative structure remains broadly the same, even as the constructions themselves appear quite different. For this reason, we shall outline this structure here, before examining the specific proofs.

We begin by demonstrating that a grid G admits a manifold M . To show so, we identify the regions R_1, \dots, R_k that partition $V(G) \setminus M$. In our diagrams, these regions are represented by the volumes enclosed by three perpendicular blue, green, and red walls. We then identify a proper unfolding H of M and show that H admits a lethal set A , where $|A| = \text{SA}(G)$. Finally, we apply corollary 4.7 to prove that G is perfect.

Construction 4.10. *All $(a, 3, 2)$ grids with $a \equiv 0 \pmod{6}$ are perfect.*

Proof. Let G be an $(a, 3, 2)$ grid with $a \equiv 0 \pmod{6}$, and let M be a manifold of G and H be its proper unfolding (see figure 4.7). Observe that M is indeed a manifold: it partitions $V(G) \setminus M$ into two sets R_1 and R_2 , both bounded by mutually orthogonal red, green, and blue faces (see figure 4.7). Furthermore, note that H is obtained from M by cutting along seams between red and green faces, and flattening the figure. It follows that H is a proper unfolding of G . We show that H admits a perfect lethal set.

Consider the initial infection A of H illustrated in figure 4.8. Observe that A infects all vertices of H by lemma 4.1, with the exception of two regions on the far left and far right. However, note that upon refolding, the two cells marked with an “X” in H represent the same cell in G . This is sufficient to infect the remaining regions of H , and by corollary 4.7, A is lethal on G . Finally, a simple calculation reveals that $|A|$ matches the surface area bound, and therefore is perfect.

We can extend this construction in the x direction by inserting the repeated structure of six columns; this augmentation percolates by lemma 4.1 and agrees with the

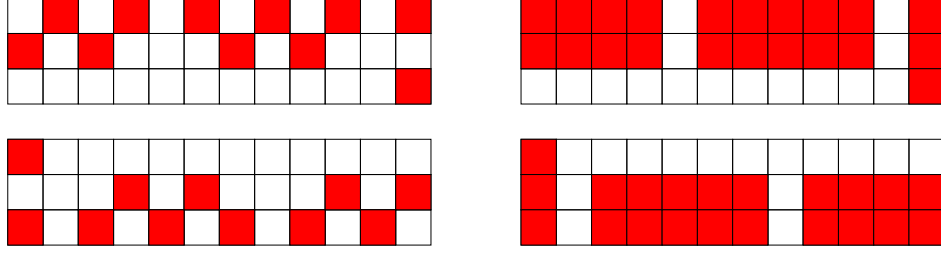
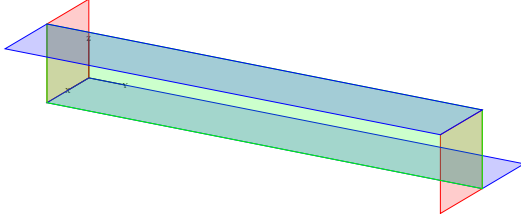
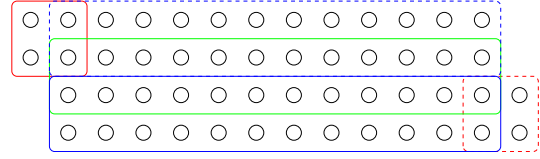


Figure 4.6: A perfect percolating set for $(3, 12, 2)$.



(a) A manifold of $G = (3, 12, 2)$.



(b) A proper unfolding of G .

Figure 4.7: A proper unfolding of $G = (3, 12, 2)$. Colored rectangles indicate faces of G . Dashed lines indicate that cells appear on different layers.

surface area bound for all larger grids. This completes the proof. \square

Construction 4.11. All $(a, 3, 2)$ grids with $a \equiv 3 \pmod{6}$ are perfect.

Proof. (This construction is the same as the previous one, except the the final four columns are augmented slightly to accommodate the $0 \pmod{3}$ requirement. Instead of deriving a proper unfolding, it is probably easier to simply show that this small change is sufficient to guarantee lethality, and agrees with the S.A. bound.) \square

Construction 4.12. All $(a, b, 2)$ grids with $a, b \in \{2, 5\} \pmod{6}$, $a \not\equiv b \pmod{6}$, and $a, b > 2$ are perfect.

Proof. Let G be an $(a, b, 2)$ grid with $a, b \in \{2, 5\} \pmod{6}$ and $a \not\equiv b \pmod{6}$, and let M be a manifold of G and H be its proper unfolding (figure 4.10). Note that M partitions the vertices of $V(G) \setminus M$ into two disjoint sets R_1 and R_2 , both bounded by mutually orthogonal red, green, and blue faces. Note, also, that H is obtained from M by cutting along seams between red and green faces, and flattening the figure. Therefore, H is a proper unfolding of G . We show that H admits a perfect lethal set.

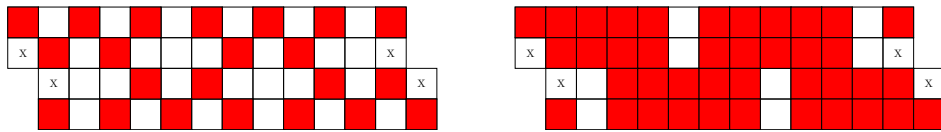


Figure 4.8: A percolating set on the proper unfolding of $G = (3, 12, 2)$.

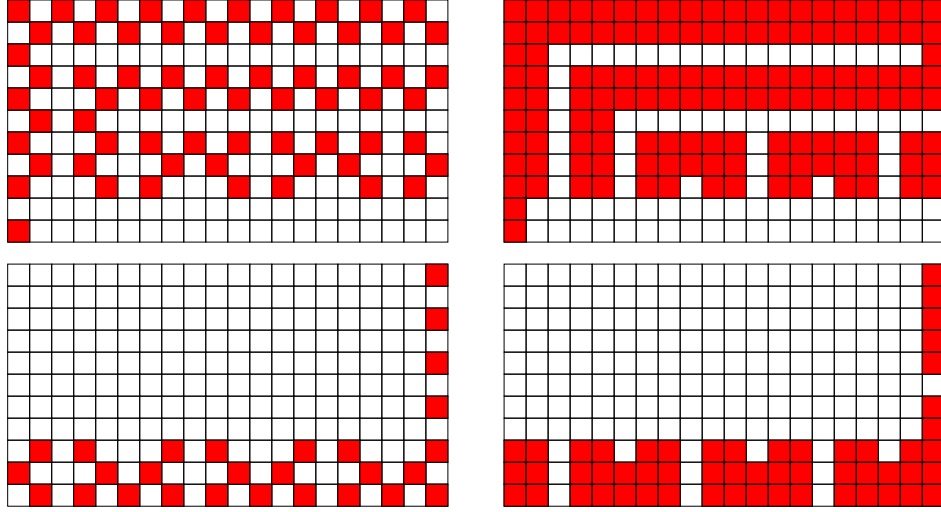
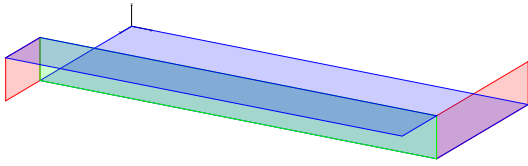
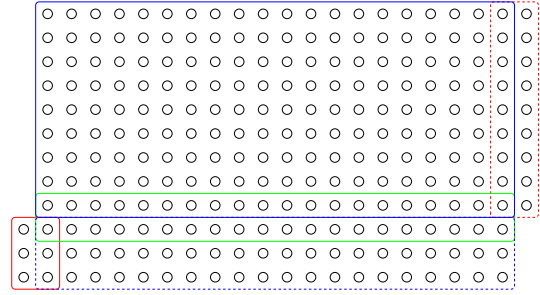


Figure 4.9: A perfect percolating set for $(11, 20, 2)$.



(a) A manifold of $G = (11, 20, 2)$.



(b) A proper unfolding of G .

Figure 4.10: A proper unfolding of $G = (11, 20, 2)$. Colored rectangles indicate faces of G . Dashed lines indicate that cells appear on different layers.

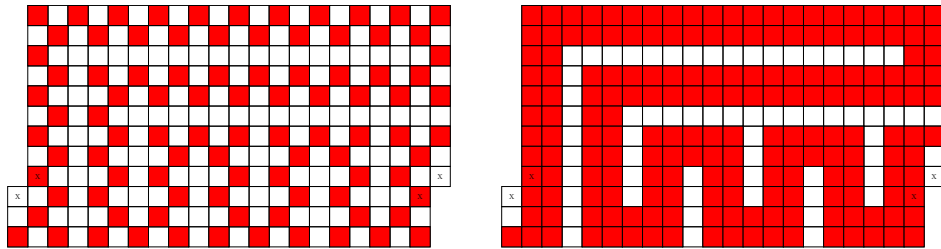


Figure 4.11: A percolating set on the proper unfolding of $G = (11, 20, 2)$.

Consider the initial infection A of H as shown in figure 4.11. By lemma 4.1, A infects all vertices of H , with the exception of two regions on the left- and right-most sides of the grid. However, note that the vertices labeled “X” in figure 4.11 represent that same vertex in G . This permits A to infect the remaining healthy vertices, thereby proving that A is lethal on H . By corollary 4.7, A is lethal on G . Finally, a simple calculation shows that $|A|$ satisfies the surface area bound on G , and so A is perfect.

The above construction holds for $a \geq 5$ and $b \geq 8$. It can be extended in the x direction by inserting a block of width 6, representing the repeating vertical snaking pattern. Similarly, it can be extended in the y direction by inserting a block of height 6, representing the horizontal snaking pattern. Both such augmentations spawn infections that satisfy the conditions of lemma 4.1, and a simple calculation reveals that they agree with the surface area bound. This concludes the proof. \square

Construction 4.13. *All $(a, b, 2)$ grids with $a, b \in \{0, 3\} \pmod{6}$ and $a \not\equiv b \pmod{6}$ are perfect.*

Proof. Consider the $(21, 12, 2)$ grid G shown in figure 4.12. Let H be a unfolding of G (figure 4.13). Observe that H is proper: three mutually orthogonal faces of G_1 are shown by blue, green and dashed red regions, and mutually orthogonal faces of G_2 are shown by the red, green and dashed blue regions. We show that H admits a lethal set of size $\text{S.A.}(12, 21, 2) = 106$. Consider such a set, as shown in figure 4.14. (Observe that this is the same set as shown in figure 4.12.) By lemma 4.1, this set percolates with the exception of two C_4 s in the top and bottom of the grid. However, notice that one of these cells is a duplicate of an already infected cell. (This duplication is a consequence of the proper unfolding of G .) Therefore, H admits a lethal set, and by corollary 4.7, G is perfect.

For all larger grids, observe that the snaking corridor in the left side G can be extended by multiples of 6 in both the x and y directions. These resulting grid still percolates under lemma 4.1. A simple calculation verifies that such an alteration produces initial infections at the surface area bound. \square

4.5 Thickness 3

Construction 4.14. *All $(a, b, 3)$ grids G with $a \equiv 3 \pmod{6}$ and $b \equiv 1 \pmod{2}$ are perfect.*

Proof. Consider the grid $H = (a + 2, b + 2, 1)$, and observe that such a grid admits an optimal percolating set by construction 4.9. Note that

$$\text{SA}(a, b, 3) = \lceil \text{SA}(a + 2, b + 2, 1) \rceil - 3.$$

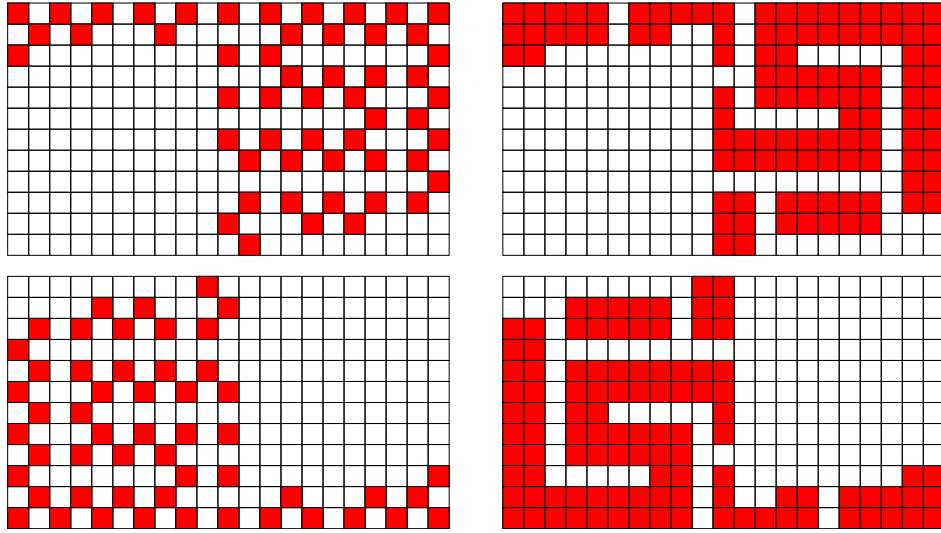


Figure 4.12: A perfect percolating set for $(12, 21, 2)$.

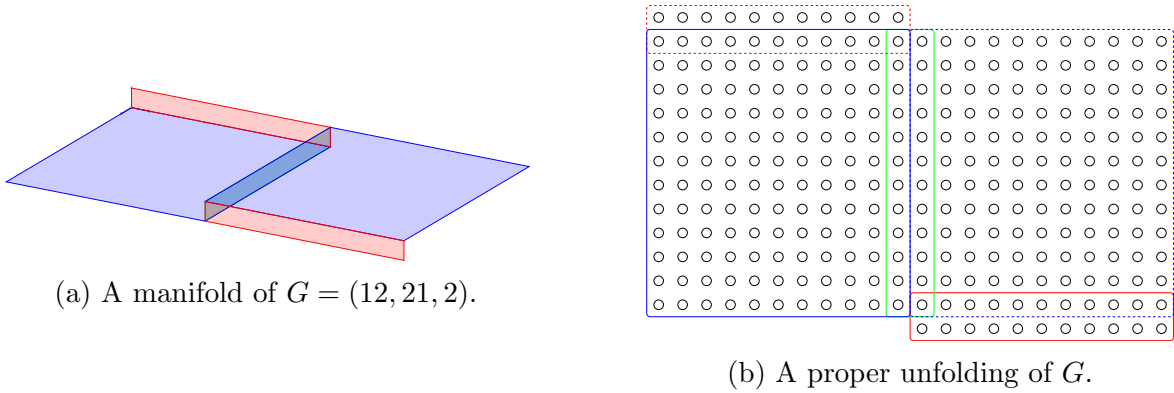


Figure 4.13: A proper unfolding of $G = (12, 21, 2)$. Colored rectangles indicate faces of G . Dashed lines indicate that cells appear on different layers.

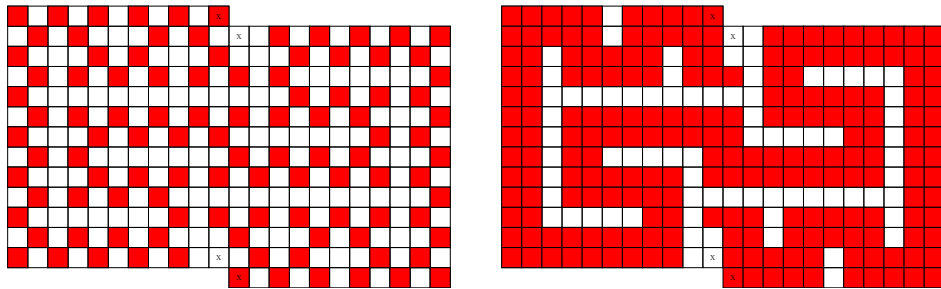


Figure 4.14: A percolating set on the proper unfolding of $G = (12, 21, 2)$.

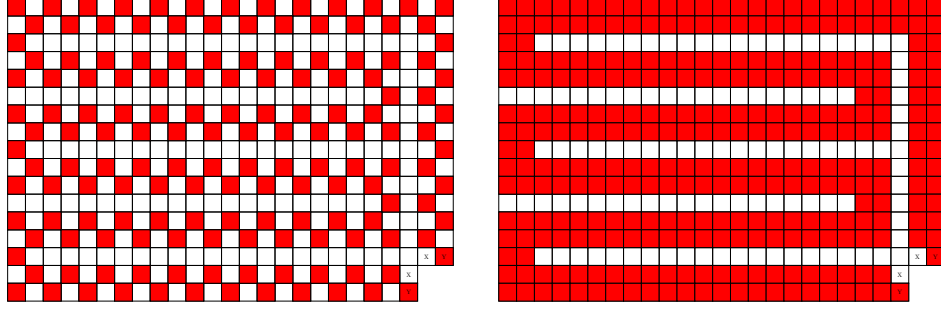
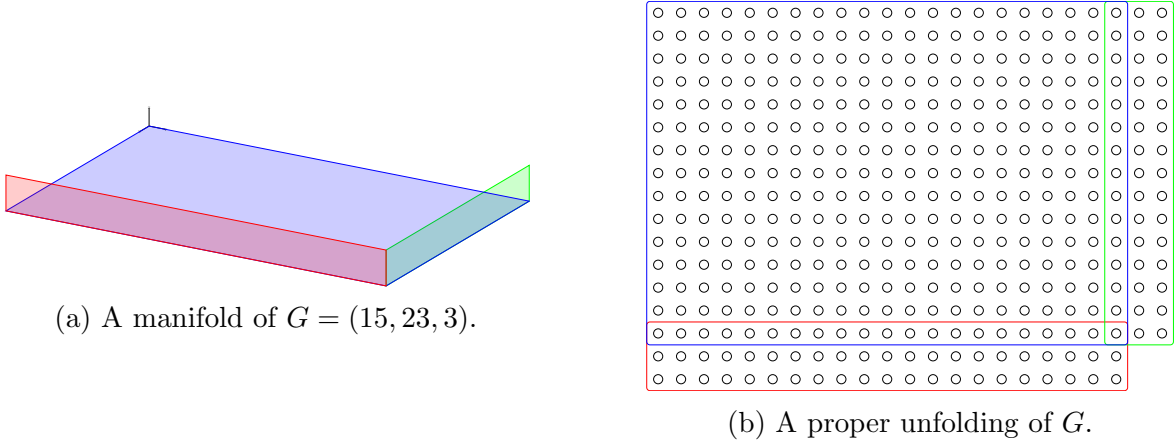


Figure 4.15: A percolating set on the proper unfolding H' of $G = (15, 23, 3)$.



(a) A manifold of $G = (15, 23, 3)$.

(b) A proper unfolding of G .

Figure 4.16: A proper unfolding of $G = (15, 23, 3)$. Colored rectangles indicate faces of G .

We show that an unfolding of G can be obtained from a simple augmentation of H . Let H' be the grid obtained by deleting the four vertices in the bottom, right-most corner of H (see figure 4.15). Consider the folding pattern illustrated in figure 4.16, and observe that the pairs of vertices adjacent to the deleted region are duplicates of each other. (In other words, consider folding up the red and green regions in figure 4.16, and notice that this operation causes vertices to overlap.) Taking this into account, the unfolding of G percolates by lemma 4.1. Since H admits an optimal percolating set of size $\lceil \text{SA}(a + 2, b + 2, 1) \rceil$, and precisely 3 of the vertices deleted from H to obtain H' were infected, it follows that the unfolding of G percolates at the lower bound. Finally, by lemma 4.7, since the unfolding of G is proper and percolates at the lower bound, G is perfect. \square

4.6 Individual constructions

In this section, we diagram lethal set constructions for single grids. The initial infection A is colored red, and all other cells are labeled with the time t that they are first

	1		1	
1		1	2	3

3	2	1		1
	1		1	

Figure 4.17

infected.

Construction 4.15. *The grid $(5, 2, 2)$ is perfect.*

Proof. See figure 4.17.

□

Construction 4.16. *The grid $(5, 5, 5)$ is perfect.*

Proof. See figure 4.18.

□

Construction 4.17. *The grid $(8, 5, 5)$ is perfect.*

Proof. See figure 4.19.

□

20	19	18	17	
9	8	7		1
	1		1	
11	8	1	6	7
12	9		7	8

19	18	17	16	15
	1	6	7	8
1		1	4	5
10	7		5	6
11	8	1	6	7

18	17		13	14
9		5	8	9
8	5	4	3	
9	6	3	2	1
10	7		1	

17	16	11	12	13
12	11	10	9	10
7	6	5		1
	5	4	1	
1		1		1

	15		1	
13	14	11		11
	15	16	17	18
1	16	17	18	19
	17	18	19	20

Figure 4.18

Chapter 5

Torus

5.1 Introduction

I know I shouldn't be working on this now but I have some ideas. We can use Benevides proof of the lower bound for the torus, which states the following:

Lemma 5.1. *Let $T = C_n \square C_m$ be the $n \times n$ torus. Let A be a lethal set on T . Then $|A| \geq \frac{nm+c}{3}$, where c is the number of components in the graph $T[\overline{A}]$.*

There are some nice observations to be made here. First, in much the same way that loss of surface area contributes to fractional increases in the surface area bound for grid graphs, the number of components can be understood to indicate sub-optimality in the torus. As a particular example, the torus $T = C_{18} \square C_{12}$ has lower bound of 72.33. This can be obtained from an optimal (but not perfect) thickness one grid construction for $(17, 11, 1)$, with an additional vertex in the bottom rightmost corner.

There's something interesting happening here. In this particular case, $T[\overline{A}]$ has three components. Assuming the best case scenario (where it has one component), we get the lower bound of 72.33. However, if we instead consider three components, the lower bound sits precisely as 73. As the construction of T simple involves adding an additional vertex to an optimal (not perfect) grid construction, it appears as though the inadequacies of the grid construction (namely, cells that are infected by 4 neighbors) somehow translate directly to inadequacies of the torus construction (multiple components in the complement).

Oh wait, is this just because the surface area argument is fundamentally an argument about the number of components in the complement? I think it is. Every time you lose surface area, you've deleted a tree from the forest (because in order to remove the final vertex in a tree, you need an inefficiency—unless the tree sits on the boundary). Therefore, it makes sense that the best solutions on the torus have exactly one component in the complement.

How does the surface area argument map to an argument about components? Knowing this should allow us to construct a lower bound on the 4D torus.

There are other questions regarding some form of algebraic or numerical equivalence between expressions for the lower bounds of tori and grids. It is clear that

Bibliography

- [1] J. Balogh and B. Bollobás. Bootstrap percolation on the hypercube. *Probability Theory and Related Fields*, 134(4):624–648, 2006.
- [2] J. Chalupa, P. L. Leath, and G. R. Reich. Bootstrap percolation on a bethe lattice. *Journal of Physics C: Solid State Physics*, 12(1):L31, 1979.